



HAL
open science

Transport study of interleukin-1 inhibitors using a human in vitro model of the blood-brain barrier

Elisabet Sjöström, Maxime Culot, Lisa Leickt, Mikael Åstrand, Erik Nordling, Fabien Gosselet, Christina Kaiser

► To cite this version:

Elisabet Sjöström, Maxime Culot, Lisa Leickt, Mikael Åstrand, Erik Nordling, et al.. Transport study of interleukin-1 inhibitors using a human in vitro model of the blood-brain barrier. *Brain, Behavior & Immunity - Health*, 2021, 16, pp.100307. 10.1016/j.bbih.2021.100307 . hal-03472272

HAL Id: hal-03472272

<https://univ-artois.hal.science/hal-03472272>

Submitted on 10 Dec 2021

HAL is a multi-disciplinary open access archive for the deposit and dissemination of scientific research documents, whether they are published or not. The documents may come from teaching and research institutions in France or abroad, or from public or private research centers.

L'archive ouverte pluridisciplinaire **HAL**, est destinée au dépôt et à la diffusion de documents scientifiques de niveau recherche, publiés ou non, émanant des établissements d'enseignement et de recherche français ou étrangers, des laboratoires publics ou privés.



Distributed under a Creative Commons Attribution - NonCommercial 4.0 International License



Full Length Article

Transport study of interleukin-1 inhibitors using a human *in vitro* model of the blood-brain barrier

Elisabet O. Sjöström^{a,1}, Maxime Culot^b, Lisa Leickt^a, Mikael Åstrand^{a,1}, Erik Nordling^a, Fabien Gosselet^b, Christina Kaiser^{a,*}

^a Swedish Orphan Biovitrum AB (publ), SE-112 76, Stockholm, Sweden

^b Univ. Artois, UR 2465, Laboratoire de la Barrière Hémato-Encéphalique (LBHE), F-62300, Lens, France

ARTICLE INFO

Keywords:

Interleukin-1
Interleukin-1 receptor antagonist
Anakinra
In vitro blood-brain barrier
Stroke
Neuronal injury
Acute brain injury
Inflammation

ABSTRACT

The proinflammatory cytokine Interleukin-1 (IL-1), with its two isoforms α and β , has important roles in multiple pathogenic processes in the central nervous system. The present study aimed to evaluate and compare the blood-to-brain distribution of anakinra (IL-1 receptor antagonist), bermekimab (IL-1 α antagonist) and canakinumab (IL-1 β antagonist).

A human *in vitro* model of the blood-brain barrier derived from human umbilical cord blood stem cells was used, where isolated CD34⁺ cells co-cultured with bovine pericytes were matured into polarized brain-like endothelial cells. Transport rates of the three test items were evaluated after 180 min incubation at concentrations 50, 250 and 1250 nM in a transwell system. We report herein that anakinra passes the human brain-like endothelial monolayer at a 4-7-fold higher rate than the monoclonal antibodies tested. Both antibodies had similar transport rates at all concentrations. No dose-dependent effects in transport rates were observed, nor any saturation effects at supraphysiological concentrations. The larger propensity of anakinra to pass this model of the human blood-brain barrier supports existing data and confirms that anakinra can reach the brain compartment at clinically relevant concentrations. As anakinra inhibits the actions of both IL-1 α and IL-1 β , it blocks all effects of IL-1 downstream signaling. The results herein further add to the growing body of evidence of the potential utility of anakinra to treat neuroinflammatory disorders.

1. Introduction

Inflammatory processes are implicated in the pathophysiology of both acute and chronic diseases affecting the central nervous system (CNS), influencing neurodegenerative processes, tissue injury, repair, and recovery. Inflammation is necessary for adequate response to injury, but responses are often exacerbated and lead to untoward effects (DiSabato et al., 2016). CNS manifestations are common in the most severe clinical phenotypes of a spectrum of autoinflammatory disorders termed cryopyrin-associated periodic syndromes (CAPS) (Sibley et al., 2012). Dysregulation of inflammatory pathways in cerebral ischemia and stroke are well documented, with sustained inflammation in subacute and chronic phases (Gerhard et al., 2005) being independently associated with worse functional outcome (Whiteley et al., 2009). Likewise, traumatic brain injury (TBI) has a large inflammatory component, where both acute and long-lasting inflammation are present (Kumar et al., 2015;

Webster et al., 2017). Also, growing evidence suggests an important role for inflammatory pathways in refractory seizure disorders and epileptogenesis (Koh et al., 2021; Vezzani et al., 2011; Webster et al., 2017).

A key mediator of inflammatory processes is the interleukin-1 (IL-1) pathway driven by the cytokines IL-1 α and IL-1 β . Both ligands act via the IL-1 type I receptor (IL-1RI), which is expressed on many cell types in the periphery as well as in the brain (Allan et al., 2005; Basu et al., 2002; Pinteaux et al., 2002). Under normal conditions, IL-1 is expressed at very low levels in the brain, but production of both IL-1 α and IL-1 β increases significantly during ischemic brain injury (Murray et al., 2015). Upregulation of IL-1 α is a critical step in the ischemia-induced inflammatory cascade (Brough and Denes, 2015), while IL-1 β production is believed to play an important role in sustaining local inflammation later in the response (Allan et al., 2005; Murray et al., 2015). A naturally occurring competitive inhibitor to IL-1 α and IL-1 β is the IL-1 receptor antagonist (IL-1Ra), which by binding to IL-1RI without inducing intracellular

* Corresponding author.

E-mail address: christina.kaiser@sobi.com (C. Kaiser).

¹ former employees of Swedish Orphan Biovitrum AB (publ).

downstream signalling, antagonizes all known functions of the two IL-1 isoforms (Dinarello, 1996; Dinarello et al., 2012; Hannum et al., 1990).

The blood-brain barrier (BBB) plays a key role in maintaining the specialized environment required for neuronal functioning. The monolayer of tightly sealed endothelial cells within brain capillaries surrounded by basement membranes, pericytes and astrocytes, together referred to as the neurovascular unit, provides a well-regulated gate for influx and efflux of molecules to cells of the brain, protecting it from systemic toxic insults, high protein loads, inflammatory mediators and immune cells (Abbott et al., 2006; Banks, 2016; Pardridge, 2012). Modelling of transport across the BBB in polarized endothelial monolayers *in vitro* allows for comparison and evaluation of transport mechanisms of relevant molecules (Cecchelli et al., 2014; Helms et al., 2016).

Anti-IL-1 molecules are an emerging treatment approach for selected CNS disorders, including stroke, TBI and seizure disorders (Helmy et al., 2014; Galea et al., 2018; Kenney-Jung et al., 2016; Koh et al., 2021). Therapeutic monoclonal antibodies targeting IL-1 β (canakinumab) and IL-1 α (bermekimab) have been developed. The recombinant version of IL-1Ra (rHuIL-1Ra), anakinra, has been in clinical use for more than 20 years. Canakinumab and anakinra are approved for several auto-inflammatory disorders, some of which have CNS manifestations, while bermekimab is being investigated in clinical trials. These three drugs differ in terms of their target (soluble factors *versus* receptor), their size (148 kDa vs 17 kDa) and their pharmacokinetic properties. It is of high relevance to understand their access to the CNS compartment and in a broader perspective, it is pertinent to consider and compare the therapeutic effects of blocking the entire IL-1 downstream pathway (through receptor blockade) versus selective cytokine neutralization.

The current study aimed to evaluate and compare the passage of canakinumab, bermekimab and anakinra into the brain using a transwell *in vitro* model of the human BBB.

2. Materials and methods

Two independent experiments were performed in this study, referred to as Experiment 1 (Exp. 1) and Experiment 2 (Exp. 2). In Exp. 1, anakinra was compared head-to-head with canakinumab and bermekimab at three concentrations. In Exp. 2, canakinumab and anakinra were explored under the same conditions as those in Exp. 1, but with an additional test item as a size control to anakinra.

2.1. Test compounds

The test items for the experiments were provided as pharmaceutical drug products (DP), for canakinumab (Ilaris®) and anakinra (Kineret®). The monoclonal antibody bermekimab (MABp1, Xilonix) was produced based on information provided in patent EP2285409 (A1/9 and A1/11). The recombinant full-length antibody was produced in ExpiCHO cells, purified and analyzed according to standard methods and formulated in NaP–NaCl buffer (pH 7.0). As a size control to anakinra, an experimentally produced single domain antibody (VHH) of Llama origin (devoid of human binding specificity or interaction partner) of approximately 15 kDa was used (D08-568P). The VHH was expressed with a C-terminal hexahistidine tag in *E. coli* periplasm using a *pelB* secretion signal peptide and purified using immobilized metal ion affinity chromatography. The VHH was fluorescently labeled with Promofluor 568 (PK PF568-1-05, PromoCell, Heidelberg, Germany), according to the manufacturer's instructions.

2.2. *In vitro* BBB model

An *in vitro* model of the human BBB using endothelial cells (ECs) derived from human umbilical cord blood stem cells (Cecchelli et al., 2014) was used to study the rate of transport of the test items. Infants' parents signed an informed consent form allowing the collection of the umbilical cord blood, in compliance with the French legislation. The

protocol was approved by the French Ministry of Higher Education and Research (CODECOH Number DC2011-1321). All experiments were performed in accordance with the approved protocol.

2.3. Cell culture

CD34⁺ cells isolated from human umbilical cord blood were differentiated into ECs, as described previously (Pedroso et al., 2011). Briefly, CD34⁺ cells were cultured in EC growth medium supplemented with serum and growth factors for 15–20 days and expanded until confluence. ECs were then trypsinized and seeded onto Matrigel coated transwell inserts (0.4 μ m pore size) at a density of 8×10^4 , and co-cultured with bovine brain pericytes for 6 days (Fig. 1A). Bovine pericytes were isolated and characterized as described in (Vandenhoute et al., 2016). Pericytes grown on the bottom well were removed prior to the experiment and replaced by empty lower chambers (Fig. 1B).

2.4. *In vitro* BBB transwell assay

Before commencement of the experiment, BLECs (on inserts) were washed twice with Ringer HEPES (RH) buffer (NaCl 150 mM, KCl 5.2 mM, CaCl₂ 2.2 mM, MgCl₂ 0.2 mM, NaHCO₃ 6 mM, glucose 2.8 mM, HEPES 5 mM). At $t = 0$ min, the test items, with or without fluorescently

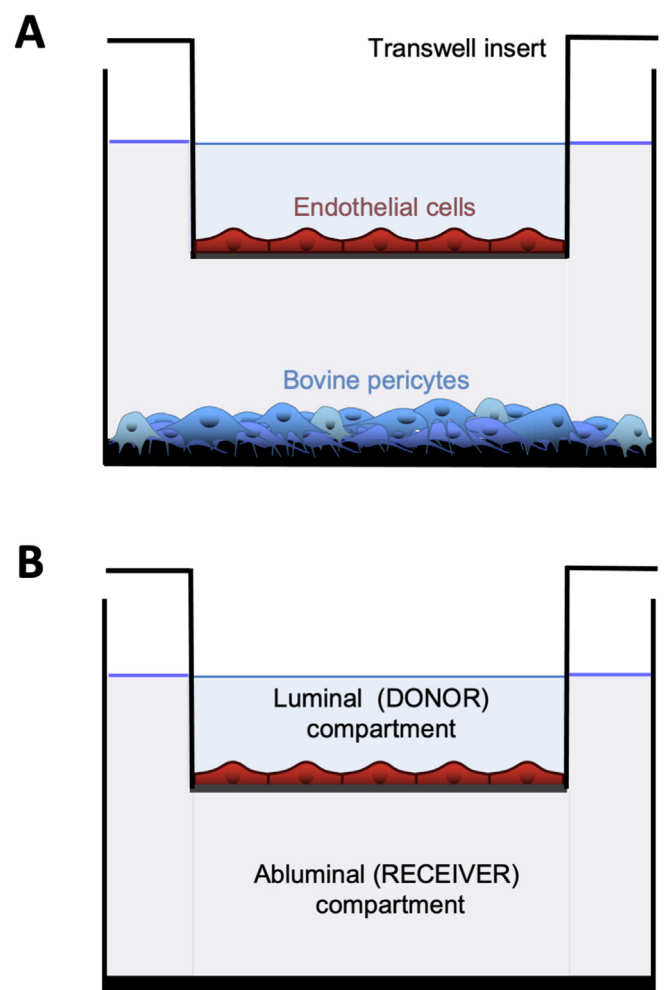


Fig. 1. Graphical representation of the human *in vitro* BBB model. (A) Co-culture of human polarized endothelial cells and bovine pericytes in the transwell system to acquire polarized BBB-like properties with a luminal and abluminal side. (B) For performing the assay, inserts with endothelial cells are washed, the bottom well is removed, and replaced by a compartment (well) without cells.

labeled human serum albumin (hSA-647; equimolar to test item (cat. # 009-600-051, Jackson ImmunoResearch Europe Ltd, Ely, United Kingdom) were added to the donor (luminal) compartment at concentrations of 50, 250 and 1250 nM (in RH buffer supplemented with 0.5% hSA and containing 1 μ M sodium fluorescein (NaF, MW 376, CAS 518-47-8, Sigma-Aldrich, Merck, Darmstadt, Germany), to verify tightness of the cell layer. Lower chambers were filled with 1.5 mL RH buffer plus 0.5% hSA. Plates were incubated at 37 °C at low shaking velocity for 3 h. At $t = 180$ min, samples were taken from the donor and receiver chambers (see Fig. 1B). BLECs were washed three times with RH buffer, scraped and lysed in 0.5 mL of radio-immunoprecipitation assay (RIPA) buffer. All experimental conditions were run in triplicate wells.

To evaluate the ability of test compounds to cross Matrigel-coated filters without cells and to control for the adsorption to plastics and/or Matrigel, the assay was also run without cells at the lowest assay concentration (50 nM). Mass balance (M.B %) was calculated from the amount of compound recovered in both compartments at the end of the experiment divided by the total amount added to the donor compartment at the start of the experiment. Samples from the assay, at $t = 0$ and $t = 180$ were immediately dispensed into 96-well plates and frozen to -70 °C. Samples were analyzed for fluorescence using a Synergy H1 (Bio-Tek, Winooski, USA) set to detect wavelengths 488, 568 and 647 and the presence of test items with customized immunoassays. Note: hSA-647 was not used in combination with the fluorescent test item (D08-568P), due to the risk of confounding fluorescence interference.

2.5. Immunoassays of test items

2.5.1. Method 1 (used in Exp. 1)

Analysis of the monoclonal antibodies (mAbs), bermekimab and canakinumab in the test samples was made using an enzyme-linked immunosorbent assay (ELISA) method established to detect the human IgG Fc domain. Briefly, microtiter plates (F96 MaxiSorp Nunc Immuno-plate 442404, ThermoFischer Scientific, Waltham, US) were coated with anti-human IgG (F(ab) specific fragment (cat # I5154, Sigma Aldrich, Merck Darmstadt, Germany), washed and blocked with 5% bovine serum albumin (BSA). Samples and standards were added, and bound protein was detected using an HRP conjugated anti-human IgG F(ab)² fragment (Sigma A2290). TMB (Sigma T0440) was used as substrate and the absorbance was measured on a SpectraMax i3 reader (Molecular Devices, San Jose, CA, USA) at 450 nm (540 nm background correction).

2.5.2. Method 2 (used in Exp. 2)

A human IgG ELISA assay from Cygnus Technologies (Southport, NC, USA; Cat #F160) was applied to measure levels of canakinumab. Samples were added to microtiter strips coated with a capture antibody and containing a horseradish peroxidase (HRP) enzyme labeled anti-hIgG antibody, resulting in the formation of a sandwich complex of solid phase antibody-human IgG-enzyme labeled antibody, followed by a TMB substrate reaction. The amount of hydrolyzed substrate was measured on a Tecan Infinite M200 Pro reader (Männedorf, Switzerland).

2.5.3. Method 3 (used for anakinra in Exp.1)

Microtiter plates were coated with anti-IL1Ra antibody (AF280 R&D Systems, Minneapolis, MN, USA) and blocked with 1% BSA. After a wash step, plates were incubated with samples or standards followed by a wash step and incubation with biotinylated anti-hIL1Ra antibody (BAF280 R&D Systems). The plates were washed and incubated with streptavidin (SA)-HRP, followed by another wash step and finally incubation with TMB (EC-Blue Enhanced, Medicago, Uppsala, Sweden). Results were read on a SpectraMax i3 reader.

2.5.4. Method 4 (used for anakinra in Exp. 2)

The second method for detection of anakinra involved an ECL (electrochemiluminescence)-based method employing an SA-coated MSD (Meso Scale Diagnostics; Rockville, MA, USA) plate that was blocked and

incubated with biotinylated anti-IL1-Ra antibody. After a wash step, diluted samples were added and incubated on the plate. After another wash step, the plates were incubated with a sulfo-tagged anti-IL-1Ra antibody solution. After a final wash step, read buffer was added to produce a chemiluminescent signal when an electrical voltage is applied. The plates were read on MSD QuickPlex SQ 120 (Meso Scale Diagnostics).

2.6. Calculation of permeability coefficients

The endothelial permeability coefficient (P_e) of the test items was calculated as described by Dehouck et al. (1992). The cleared volume was obtained by dividing the amount of test items in the receiver compartment at the end by its concentration in the donor compartment at the onset of experiment, divided by the duration of the experiment (180 min) to elicit the permeability surface area product (PS in μ L per minute). In this calculation, both the permeability of filters without cells ($PS_f = \text{insert filter} + \text{coating}$) and filters with cells ($PS_t = \text{filter} + \text{coating} + \text{ECs}$) were taken into account, according to the formula:

$$PSe = \left(\frac{1}{PS_f} + \frac{1}{PS_t} \right)^{-1}$$

PSe is the permeability surface area product of the ECs monolayer (in μ L per minute) which is divided by the surface area of the filter (S, which is 1.13 cm² for a 12-well format inserts) to generate the endothelial permeability coefficient (P_e) in centimeters per minute.

$$P_e = PSe/S$$

2.7. Analysis & statistics

As Exp. 1 and Exp. 2 were run at different time points and from different primary cells, results are not compared side by side as absolute values. Moreover, the immunoassays used to quantify the test items differed with respect to methodology, materials and location. Within each experiment, P_e values were compared with two-way ANOVA and Tukey's test of multiple comparisons for groupwise comparisons (test items). Significance threshold level was set at $p < 0.05$. Data analyses and statistics were performed using Graph Pad Prism 9 (San Diego, California, USA).

3. Results

3.1. Recovery/mass balance without cells

To ensure that passage of the test compounds was not critically limited by the filter or Matrigel coating, each test item was run in triplicate at 50 nM in well inserts and buffer, without BLECs, for 3 h. Among the tested compounds, the recovery and mass balance ranged from 88% to 101% in Exp. 1 and from 93% to 123% in Exp. 2 (Table 1). Passage of the test items, i.e. the amount diffused (%) from the upper (donor) to lower (receiver) chamber after 3 h across the inserts without cells, were in the same range between test compounds 27.3–33.6% and 19.2–26.4% for Exp. 1 and 2, respectively. The amount diffused was slightly higher for anakinra (17 kDa) than for canakinumab (148 kDa), Table 1.

3.2. Cellular integrity, permeability of NaF and hSA

Cellular tightness and consequent permeability (P_e) of the BLEC monolayer to the small integrity marker NaF was overall low and stable in both experiments, with no signs of toxicity or untoward effect of the added test items at any concentration when compared with controls without added protein (Fig. 2A and B). The two studies used different primary cell sources and reagent batches (such as serum), and consequently a clear difference in basal cell permeability was observed. Within

Table 1
Permeability to test items without cells in the transwell system.

Experiment 1		Diffused at t = 180 min (%)	Mass balance (% recovery)	Psf ($\mu\text{L} \times \text{min}^{-1}$)
Test item	Approximate MW	Mean (SD)	Mean (SD)	Mean (SD)
Anakinra	17 kDa	33.6 (9.7)	87.6 (27.6)	1.47 (0.64)
Bermekimab	148 kDa	32.5 (4.3)	101.4 (12.2)	1.35 (0.27)
Canakinumab	148 kDa	27.3 (4.2)	91.9 (10.3)	1.05 (0.23)
Experiment 2		Diffused at t = 180 min (%)	Mass balance (% recovery)	Psf ($\mu\text{L} \times \text{min}^{-1}$)
Test item	Approximate MW	Mean (SD)	Mean (SD)	Mean (SD)
Anakinra	17 kDa	26.4 (2.1)	93 (5)	1.00 (0.11)
Control D08-568P	15 kDa	24.0 (3.8)	97 (3)	0.88 (0.14)
Canakinumab	148 kDa	19.2 (11.2)	123 (35)	0.70 (0.46)

Table 1. Amount diffused (%) after 180 min, mass balance (amount recovered) and passage (or diffusion) rate of test items at 50 nM without cells (Psf). kDa, kilo daltons, MW; Molecular weight, nM; nanomolar, min; minutes, SD; standard deviation, μL ; microliters.

each of the two experiments (Exp.1 and Exp. 2), the range of the endothelial permeability to NaF (P_e to NaF) obtained in the presence or absence of the test compounds at different concentrations was narrow (Exp. 1: $0.70\text{--}1.08 \times 10^{-3} \text{ cm/min}$ and Exp 2: $0.27\text{--}0.38 \times 10^{-3} \text{ cm/min}$). We have previously validated the use of fluorescent hSA (hSA-647) as

size control in the assay system to not affect cellular integrity at any concentration used herein. Endothelial permeability (P_e) to hSA-647 when co-incubated with test items (at equimolar concentrations) was stable at all concentrations (50, 250 and 1250 nM) and in a similar range for all test item conditions (Fig. 2C and D). A slightly elevated P_e to NaF was observed in the hSA 1250 nM control (without test item co-incubation, Exp. 1, Fig. 1B “hSA-647”). This result was not observed in a parallel plate run performed at the same time from another donor (data not shown), or in Exp. 2. In Exp. 2, hSA-647 was omitted in all wells with D08-568P, to avoid the risk of fluorescence interference, and hence was not determined (ND).

3.3. Endothelial permeability of test items

In a first experiment, the difference between IL-1 targeting biologics in transport rates across the BLECs was investigated. Bermekimab and canakinumab showed very low, dose-dependent, transport rates across the endothelial monolayer at all concentrations (P_e $0.74\text{--}0.94 \times 10^{-5} \text{ cm/min}$ and P_e $0.53\text{--}0.75 \times 10^{-5} \text{ cm/min}$, respectively), Fig. 3A. The transport rate for anakinra was 5-6-fold higher than bermekimab and canakinumab (P_e $3.32\text{--}4.44 \times 10^{-5} \text{ cm/min}$; $p < 0.0001$, two-way ANOVA), with no dose-dependent effects on permeability rates (Fig. 3A). To validate the findings, the experiment was repeated with the two drugs that are used clinically, canakinumab and anakinra, as well as a non-IL-1 targeting size control (D08-568P, 15 kDa), which is devoid of specific human binding interactions. As expected, the size control behaved similarly to that of anakinra with transport rates across BLECs over 3 h at all concentrations tested (Fig. 3B), and rates of transport were in the same range for D08-568P (P_e $2.20\text{--}3.01 \times 10^{-5} \text{ cm/min}$) as for anakinra (P_e $2.85\text{--}3.14 \times 10^{-5} \text{ cm/min}$). As previously observed (Exp. 1), canakinumab had lower transport rates across BLECs compared to

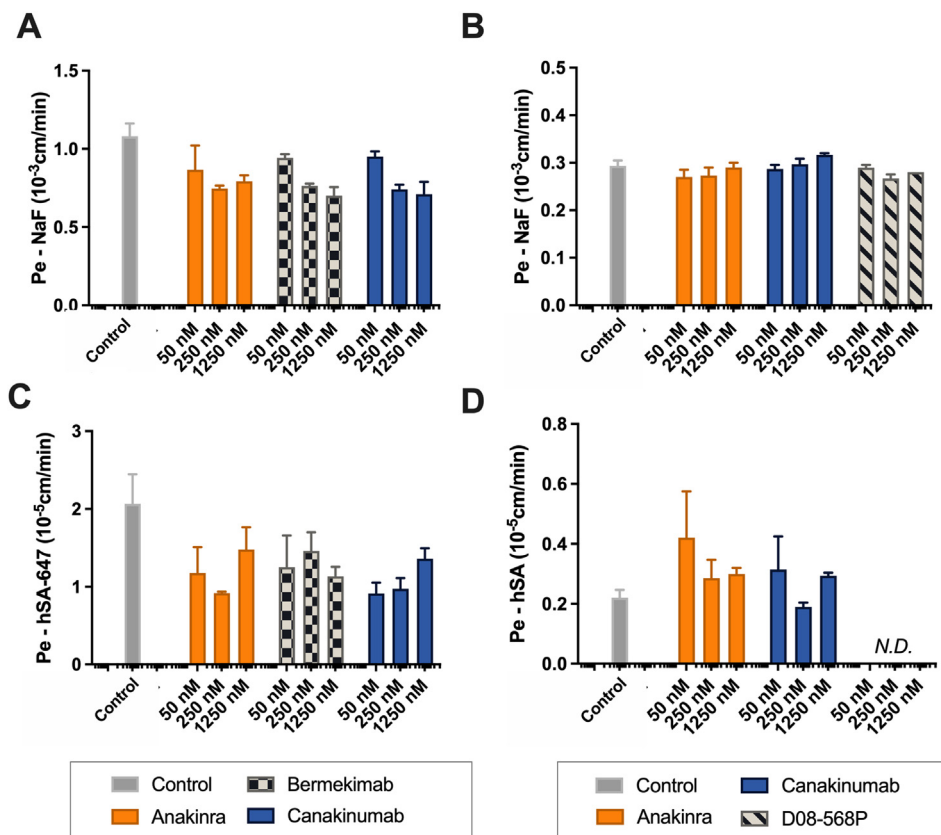


Fig. 2. Endothelial permeability (P_e) of integrity and size controls, detected by fluorometric analysis, in Experiment 1 (left panels) and Experiment 2 (right panels). (A–B) Permeability to the integrity marker sodium fluorescein (NaF) at $1 \mu\text{M}$ in all experimental conditions. (C–D) Permeability of human serum albumin Alexa-647 (hSA-647), added at equimolar concentration to test items or alone as control (1250 nM). N.D.; not determined.

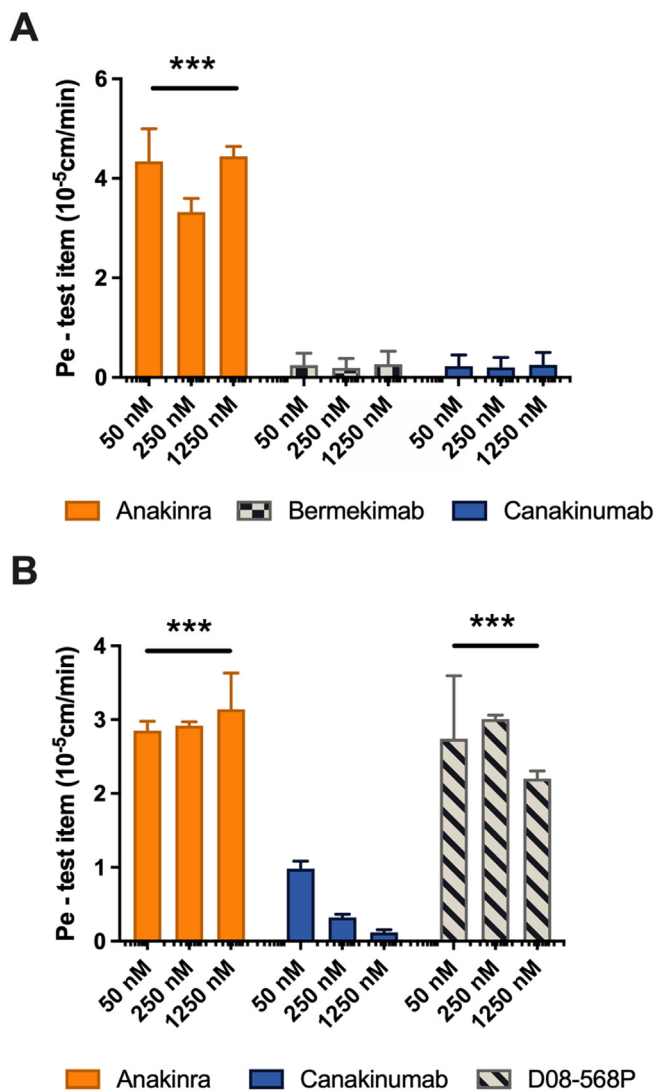


Fig. 3. Endothelial permeability (Pe) of test items at three concentrations (50, 250 and 1250 nM) as determined by specific immunoassays or fluorometric detection. (A) Experiment 1: Anakinra, bermekimab and canakinumab. (B) Experiment 2: Anakinra, canakinumab and D08-568P (size control). *** $p < 0.0001$ vs canakinumab, two-way ANOVA followed by Tukey's post-hoc for groupwise treatment effect (<0.0001).

anakinra ($p < 0.0001$ two-way ANOVA) with no signs of saturation of transport. In Exp. 2, there was a large spread in values detected in immunoassays for canakinumab, hence a suspected under- and over-estimation of certain values. As no significant concentration-dependent effects on transport rates have been observed for any test item, a comparison of the mean value for all concentrations ($n = 9$ per test item and experiment) can give data for relevant inter-assay comparisons. In Exp. 2, a 6.3-fold higher transport rate of anakinra ($Pe\ 2.97 \pm 0.46 \times 10^{-5}$ cm/min) compared to canakinumab ($Pe\ 0.47 \pm 0.40 \times 10^{-5}$ cm/min) was observed, compared to a 4.8-fold difference in Exp. 1. Of importance, transport rates of canakinumab and bermekimab were in parity with those of hSA-647 in both experiments (Fig. 2C vs Figs. 3A and 2D vs Fig. 3B). Mass balance for experiments with cells and P_{st} values are reported in Table 2.

3.4. Intracellular accumulation

At the end of each experiment, BLECs were washed, scraped and lysed in buffer. Intracellular uptake of the test items at the end of the

Table 2

Volume cleared and mass balance for test items in experiments with cells.

Experiment 1			Experiment 2		
Condition (test item)	PSt $\mu\text{L}/\text{min}$ (SD)	Mass balance (%) recovery)	Condition (test item)	PSt $\mu\text{L}/\text{min}$ (SD)	Mass balance (%) recovery)
Anakinra 50 nM	0.047 (0.012)	56 (18)	Anakinra 50 nM	0.031 (0.002)	83 (3)
Anakinra 250 nM	0.037 (0.005)	99 (1)	Anakinra 250 nM	0.032 (0.001)	94 (1)
Anakinra 1250 nM	0.049 (0.004)	69 (6)	Anakinra 1250 nM	0.034 (0.001)	99 (5)
Bermekimab 50 nM	0.011 (0.003)	85 (8)	D08-568P 50 nM	0.030 (0.016)	96 (4)
Bermekimab 250 nM	0.009 (0.003)	96 (1)	D08-568P 250 nM	0.033 (0.001)	92 (2)
Bermekimab 1250 nM	0.008 (0.002)	93 (5)	D08-568P 1250 nM	0.024 (0.002)	95 (5)
Canakinumab 50 nM	0.006 (0.002)	92 (7)	Canakinumab 50 nM	0.011 (0.002)	125 (5)
Canakinumab 250 nM	0.007 (0.002)	93 (4)	Canakinumab 250 nM	0.004 (0.001)	241 (41)
Canakinumab 1250 nM	0.008 (0.001)	87 (2)	Canakinumab 1250 nM	0.001 (0.001)	114 (5)

Table 2. Volume cleared from donor to receiver compartment per minute (P_{st}) and mass balance expressed as percentage (%) recovery of test item at the end of experiment., nM; nanomolar, min; minutes, SD; standard deviation, μL ; microliters.

experiments was overall low. In Exp. 1, all test items showed an intracellular accumulation of less than 0.1% (0.03–0.08%) of the added compound (Fig. 4A). In Exp. 2, the intracellular accumulation for anakinra and canakinumab was in a similar range (0.02–0.14%), and values were below the limit of detection (LOD). Interestingly, accumulation was higher for the size control D08-568P (0.72–0.86%), Fig. 4B.

4. Discussion

To gain an understanding of gross transport characteristics of different pharmaceuticals employed in the clinic towards the interleukin-1 pathway, an unbiased evaluation of directional transport was performed in a human *in vitro* BBB system, namely BLECs. To our knowledge, this is the first reported comparative study of three clinically relevant drugs targeting the IL-1 pathway. Anakinra, a recombinant form of the human IL-1Ra (rHuIL-1Ra; 17 kDa), was compared with the two recombinant human monoclonal IgGs (148 kDa) that block IL-1 α (bermekimab) and IL-1 β (canakinumab). Results from the present study demonstrate that anakinra displays the highest rate of transport across the BLECs, from the luminal to the abluminal compartment. The transport rate provides estimates for a theoretical comparison of brain exposure after systemic dosing between the drugs. Doses tested herein were in relevant ranges for a pharmacological C_{max} in plasma. For canakinumab, C_{max} in patients (adults, 150 mg dose) is reported to be 16 ± 3.5 $\mu\text{g}/\text{mL}$ (corresponding to 110 nM) occurring at 7 days (Chakraborty et al., 2012). Anakinra has a reported C_{max} of 3.6 $\mu\text{g}/\text{mL}$ (range 0.7–8.5) $\mu\text{g}/\text{mL}$ (corresponding to 211 nM) occurring after 3–7 h (Kineret SPC “Kineret Summary of Product Characteristics,” 2020). Despite apparent differences in pharmacokinetic profiles between anakinra and mAbs, a C_{max} reflects the concentration exposed to the BBB and hence, indicates the amounts readily available for brain uptake.

Brain exposure of systemically dosed biologics is inherently difficult to predict in both preclinical and clinical settings. First, samples of brain interstitial fluid in the clinic are not readily available, except for microdialysates in neurocritical care (e.g. cerebral microdialysis in TBI and subarachnoid hemorrhage). Second, although there is exchange between brain interstitial fluid and cerebrospinal fluid (CSF), CSF composition does not fully reflect the contents of the brain interstitium and *vice versa*

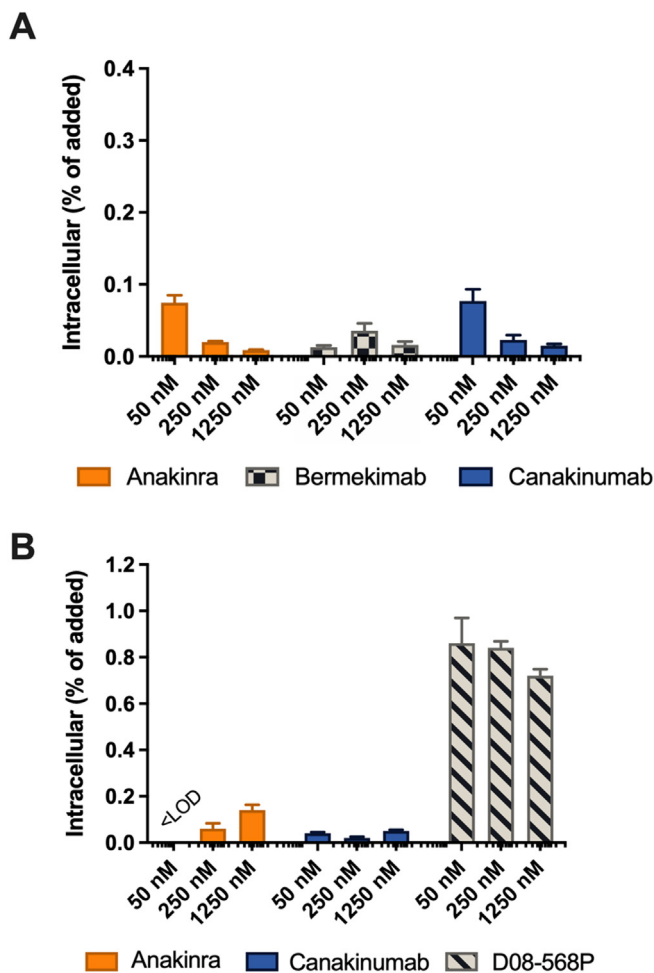


Fig. 4. Intracellular accumulation of test items, as detected from cell lysate of scraped cells diluted in buffer. (A) Experiment 1: Anakinra, bermekimab and canakinumab. (B) Experiment 2: Anakinra, D08-568P, and canakinumab. (<LOD: Below limit of detection).

(Banks, 2016; Hladky and Barrand, 2014). For molecules devoid of active transport mechanisms, size and lipophilicity are major determinants of brain passage (Banks, 2016; Pardridge, 2012). To compare the impact of size *versus* specific transport mechanisms of anakinra, a small recombinant protein with no human target, D08-568P (15 kDa) was compared side-by-side to anakinra. As very similar transport rates were found between the two compounds, no major influence of active transport can be interpreted from the present study. Previous studies have suggested that the transport of IL-1Ra across the BBB was mediated through receptor-mediated transcytosis (Skinner et al., 2009). Although the present study has no mechanistic approach to refute this hypothesis, we also have no data to support it. IL-1RI is widely expressed on many cell types of the brain, including the cerebrovasculature (Basu et al., 2002; Konzman et al., 2004; Pinteaux et al., 2002), but has not been implicated in mediating transcytosis of its ligands. Large proteins such as antibodies (IgGs), are estimated to enter the brain compartment in a range of 0.1–1% (Banks, 2016; Pardridge, 2012; Shah and Betts, 2013). In congruence with previously reported findings *in vivo* (Poduslo et al., 1994), albumin and IgG showed similarly low transport rates across the BLECs, also in the present study. The monoclonal antibodies used herein have, to our knowledge, not hitherto been studied specifically regarding their exposure or transport to brain. It can be assumed that both canakinumab and bermekimab follow the same principles of distribution as other IgGs (endogenous and therapeutic) (Keizer et al., 2010; Shah and Betts, 2013). A plausible contribution of circulating levels of their

respective ligands (IL-1 α and IL-1 β) should not be neglected in a hyper-inflammatory state, and hence could affect the free *versus* the bound state of the mAbs.

The transport of IL-1Ra into rodent brain *in vivo* has been previously demonstrated (Greenhalgh et al., 2010; Gutierrez et al., 1994). Further indirect evidence of central exposure comes from preclinical stroke models where systemically administered rHuIL-1Ra was found to be neuroprotective and limited functional impairment (Clark et al., 2007; Pradillo et al., 2017; Relton et al., 1996). Furthermore, clinical reports show that systemically administered rHuIL-1Ra resulted in peak CSF levels of around 100 ng/ml (Clark et al., 2007; Galea et al., 2010; Gueorguieva et al., 2008). However, it is important to consider that CSF exposure is merely a pseudomarker of brain exposure and does not confirm actual brain exposure (Pardridge, 2012). Brain exposure to anakinra has been documented in TBI, where microdialysis has been employed during neurocritical care. In a phase II randomized clinical study in TBI patients, rHuIL-1Ra was administered once daily and detected in the brain microdialysate (mean level 150–200 pg/mL; endogenous control levels 10–20 pg/mL) (Helmy et al., 2014). In another study, endogenous IL-1Ra was reported in the microdialysate of TBI patients, with increasing concentrations in relation to IL-1 α and IL-1 β , yielding a positive impact on edema, intracranial pressure and outcome (Hutchinson et al., 2007).

Intriguingly, in patients with febrile-infection related epilepsy syndrome (FIRES), a refractory status epilepticus affecting children and young adults without active epilepsy and without clear structural, toxic, or metabolic cause, several recent case reports have demonstrated positive outcome measures after treatment with rHuIL-1Ra. The syndrome is highly refractory and resistant to conventional treatment, resulting in high mortality and severe neurologic morbidity in those who do survive (Payne et al., 2020). Inflammatory processes are believed to be decisively involved (Kenney-Jung et al., 2016; Sakuma et al., 2015). A growing body of evidence shows encouraging long-lasting effects of IL-1 inhibition through rHuIL-1Ra (DeSena et al., 2018; Kenney-Jung et al., 2016; Westbrook et al., 2019). Of particular significance is evidence showing that certain responders to rHuIL-1Ra treatment have a functional deficit in the production of endogenous IL-1Ra, thus providing direct mechanistic support for the hypothesis (Clarkson et al., 2019).

Canakinumab and anakinra are both approved for the treatment of diseases within the autoinflammatory syndrome CAPS. The divergent treatment outcomes of the two drugs with regards to patients with CNS manifestations, with anakinra being possibly more effective, are interesting in view of the results obtained in this study (Sibley et al., 2012, 2015).

Many CNS disorders have an integral inflammatory component and correspondingly show a compromised BBB, where both IgG and smaller proteins can enter the brain parenchyma (Liebner et al., 2018). In a preclinical study where rHuIL-1Ra was dosed systemically in rat, distribution of the molecule was found within the infarct area overlapping that of IgG-positivity, indicating passage over a compromised BBB (Greenhalgh et al., 2010). In epilepsy, focal BBB compromise is present within ictogenic areas (Löscher and Friedman, 2020; Vezzani et al., 2011), and thus a higher entrance of blood-borne proteins is expected. Given that therapeutic intervention in brain injury or severe epilepsy would face a compromised BBB, it is important to consider that the rates of passage reported herein merely represent a theoretical modelling of an intact BBB.

Antagonism of the IL-1 pathway is an attractive therapeutic strategy for several CNS indications. Expression of IL-1 is usually low in the brain but is rapidly induced upon brain injury (Allan et al., 2005). IL-1 β has long been considered the major effector cytokine of the two IL-1 isoforms, with documented untoward effects in stroke. Levels of IL-1 β have been correlated with worsening of infarct severity (Yamasaki et al., 1995), and genetic deletion of IL-1 β and IL-1R1 have resulted in positive or neuroprotective outcomes in murine stroke model (Boutin et al., 2001; Lazovic et al., 2005). In TBI, untoward effects of IL-1 β are supported by

preclinical findings (Clausen et al., 2011; Ozen et al., 2020). In congruence, administration of rHuIL-1Ra in preclinical TBI models and to patients have shown favourable effects such as reduced neuroinflammation and improved cognition (Helmy et al., 2014; Newell et al., 2018).

IL-1 α has been less studied in relation to CNS disease and outcome but evidence for its role in the tissue response to stroke has emerged (Brough and Denes, 2015; Luheshi et al., 2011) and a recent experimental study demonstrated that inhibition of IL-1 α alone contributed to reduced infarct size and improved neurological performance after middle cerebral artery occlusion in mice (Liberale et al., 2020). Several independent preclinical studies in models of ischemic stroke, intracerebral hemorrhage (ICH) and acute subarachnoid hemorrhage (aSAH), have reported beneficial effects of rHuIL-1Ra *in vivo*, in both rats and mice, effects confirmed in cross-laboratory studies and meta-analyses (Maysami et al., 2015; McCann et al., 2016). Correspondingly, clinical studies of systemic administration of rHuIL-1Ra have been undertaken in acute ischemic stroke and aSAH (Clark et al., 2007; Emsley et al., 2005; Galea et al., 2018). Encouraging data have emerged, and rHuIL-1Ra is currently being tested in a Phase 3 multi-centre trial in aSAH (NCT03249207), and in a Phase 2 multi-centre trial in ICH (NCT03737344).

5. Conclusion

We report a comparative study of three clinically relevant drugs targeting the IL-1 pathway and their transport rate across an *in vitro* model of the human BBB. Concordant evidence from both preclinical and clinical settings have shown that rHuIL-1Ra reaches the brain at experimentally therapeutic concentrations and has proof-of-concept biologic efficacy, while no such studies have been reported for the IL-1 α and IL-1 β neutralizing antibodies. Shown in this *in vitro* study, rHu-IL1Ra has a larger propensity to pass an *in vitro* model of the human BBB, compared to monoclonal antibodies. Importantly, rHu-IL1Ra inhibits the actions of both IL-1 isoforms and consequently blocks all downstream signalling. IL-1 α is an early and important initiator of inflammatory processes in conjunction with acute brain injury while IL-1 β propagates the inflammatory cascade and induces the production of several downstream effector molecules. Increasing evidence in support of a causative relationship between persistent, detrimental inflammation and CNS related disorders underscores the potential for targeting the IL-1 system in the brain, to alleviate symptoms and improve clinical outcomes.

Declaration of competing interest

CK, LL, EN are current employees of Swedish Orphan Biovitrum AB (publ), EOS is a former employee and current consultant contracted by Swedish Orphan Biovitrum AB (publ), MÅ is a former employee of Swedish Orphan Biovitrum AB (publ). CK, LL, EN, EOS are shareholders of Swedish Orphan Biovitrum AB (publ). MC and FG have been contracted for performing the study at LBHE (UA) by Swedish Orphan Biovitrum AB (publ).

Acknowledgements

The authors are grateful for excellent technical performance of the *in vitro* model by Lucie Dehouck and Emmanuel Sevin (LBHE). Also, at Swedish Orphan Biovitrum, the authors acknowledge excellent technical work to produce and prepare proteins, Kristin Strandberg and Robert Svensson, and for bioanalytical excellence in assay setup and analysis by Lars Bergquist.

References

Abbott, N.J., Rönnbäck, L., Hansson, E., 2006. Astrocyte–endothelial interactions at the blood–brain barrier. *Nat. Rev. Neurosci.* 7, 41–53. <https://doi.org/10.1038/nrn1824>.
Allan, S.M., Tyrrell, P.J., Rothwell, N.J., 2005. Interleukin-1 and neuronal injury. *Nat. Rev. Immunol.* 5, 629–640. <https://doi.org/10.1038/nri1664>.

Banks, W.A., 2016. From blood–brain barrier to blood–brain interface: new opportunities for CNS drug delivery. *Nat. Rev. Drug Discov.* 15, 275–292. <https://doi.org/10.1038/nrd.2015.21>.
Basu, A., Krady, J.K., O'Malley, M., Styren, S.D., DeKosky, S.T., Levison, S.W., 2002. The type 1 interleukin-1 receptor is essential for the efficient activation of microglia and the induction of multiple proinflammatory mediators in response to brain injury. *J. Neurosci.* 22, 6071–6082. <https://doi.org/10.1523/jneurosci.22-14-06071.2002>.
Boutin, H., LeFeuvre, R.A., Horai, R., Asano, M., Iwakura, Y., Rothwell, N.J., 2001. Role of IL-1 α and IL-1 β in ischemic brain damage. *J. Neurosci.* 21, 5528–5534. <https://doi.org/10.1523/jneurosci.21-15-05528.2001>.
Brough, D., Denes, A., 2015. Interleukin-1 α and brain inflammation. *IUBMB Life* 67, 323–330. <https://doi.org/10.1002/iub.1377>.
Cecchelli, R., Aday, S., Sevin, E., Almeida, C., Culot, M., Dehouck, L., Coisne, C., Engelhardt, B., Dehouck, M.-P., Ferreira, L., 2014. A stable and reproducible human blood–brain barrier model derived from hematopoietic stem cells. *PLoS One* 9, e99733. <https://doi.org/10.1371/journal.pone.0099733>.
Chakraborty, A., Tannenbaum, S., Rordorf, C., Lowe, P.J., Floch, D., Gram, H., Roy, S., 2012. Pharmacokinetic and pharmacodynamic properties of canakinumab, a human anti-interleukin-1 β monoclonal antibody. *Clin. Pharmacokinet.* 51, e1–e18. <https://doi.org/10.2165/11599820-000000000-00000>.
Clark, S.R., McMahon, C.J., Gueorgieva, I., Rowland, M., Scarth, S., Georgiou, R., Tyrrell, P.J., Hopkins, S.J., Rothwell, N.J., 2007. Interleukin-1 receptor antagonist penetrates human brain at experimentally therapeutic concentrations. *J. Cerebr. Blood Flow Metabol.* 28, 387–394. <https://doi.org/10.1038/sj.cbfm.9600537>.
Clarkson, B.D.S., LaFrance-Corey, R.G., Kahoud, R.J., Farias-Moeller, R., Payne, E.T., Howe, C.L., 2019. Functional deficiency in endogenous interleukin-1 receptor antagonist in patients with febrile infection-related epilepsy syndrome. *Ann. Neurol.* 85, 526–537. <https://doi.org/10.1002/ana.25439>.
Clausen, F., Hånell, A., Israelsson, C., Hedin, J., Ebendal, T., Mir, A.K., Gram, H., Marklund, N., 2011. Neutralization of interleukin-1 β reduces cerebral edema and tissue loss and improves late cognitive outcome following traumatic brain injury in mice. *Eur. J. Neurosci.* 34, 110–123. <https://doi.org/10.1111/j.1460-9568.2011.07723.x>.
Dehouck, M., Jolliet-Riand, P., Brée, F., Fruchart, J., Cecchelli, R., Tillement, J., 1992. Drug transfer across the blood–brain barrier: correlation between *in vitro* and *in vivo* models. *J. Neurochem.* 5, 1790–1797.
DeSena, A.D., Do, T., Schulert, G.S., 2018. Systemic autoinflammation with intractable epilepsy managed with interleukin-1 blockade. *J. Neuroinflammation* 15 (38). <https://doi.org/10.1186/s12974-018-1063-2>.
Dinarello, C., 1996. Biologic basis for interleukin-1 in disease. *Blood* 87, 2095–2147. <https://doi.org/10.1182/blood.v87.6.2095.bloodjournal8762095>.
Dinarello, C.A., Simon, A., Meer, van der, J.W.M., 2012. Treating inflammation by blocking interleukin-1 in a broad spectrum of diseases. *Nat. Rev. Drug Discov.* 11, 633–652. <https://doi.org/10.1038/nrd3800>.
DiSabato, D.J., Quan, N., Godbout, J.P., 2016. Neuroinflammation: the devil is in the details. *J. Neurochem.* 139, 136–153. <https://doi.org/10.1111/jnc.13607>.
Emsley, H., Smith, C.J., Georgiou, R.F., Vail, A., Hopkins, S.J., Rothwell, N.J., Tyrrell, P.J., 2005. A randomised phase II study of interleukin-1 receptor antagonist in acute stroke patients. *J. Neurol. Neurosurg. Psychiatr.* 76 (1366). <https://doi.org/10.1136/jnnp.2004.054882>.
Galea, J., Ogungbenro, K., Hulme, S., Greenhalgh, A., Aarons, L., Scarth, S., Hutchinson, P., Grainger, S., King, A., Hopkins, S.J., Rothwell, N., Tyrrell, P., 2010. Intravenous anakinra can achieve experimentally effective concentrations in the central nervous system within a therapeutic time window: results of a dose-ranging study. *J. Cerebr. Blood Flow Metabol.* 31, 439–447. <https://doi.org/10.1038/jcbfm.2010.103>.
Galea, J., Ogungbenro, K., Hulme, S., Patel, H., Scarth, S., Hoadley, M., Illingworth, K., McMahon, C.J., Tzerakis, N., King, A.T., Vail, A., Hopkins, S.J., Rothwell, N., Tyrrell, P., 2018. Reduction of inflammation after administration of interleukin-1 receptor antagonist following aneurysmal subarachnoid hemorrhage: results of the Subcutaneous Interleukin-1Ra in SAH (SCIL-SAH) study. *J. Neurosurg.* 128, 515–523. <https://doi.org/10.3171/2016.9.jns16615>.
Gerhard, A., Schwarz, J., Myers, R., Wise, R., Banati, R.B., 2005. Evolution of microglial activation in patients after ischemic stroke: a [¹¹C](R)-PK11195 PET study. *Neuroimage* 24, 591–595. <https://doi.org/10.1016/j.neuroimage.2004.09.034>.
Greenhalgh, A., Galea, J., Dénes, A., Tyrrell, P., Rothwell, N., 2010. Rapid brain penetration of interleukin-1 receptor antagonist in rat cerebral ischaemia: pharmacokinetics, distribution, protection. *Br. J. Pharmacol.* 160, 153–159. <https://doi.org/10.1111/j.1476-5381.2010.00684.x>.
Gueorgieva, I., Clark, S.R., McMahon, C.J., Scarth, S., Rothwell, N.J., Tyrrell, P.J., Tyrrell, P.J., Hopkins, S.J., Rowland, M., 2008. Pharmacokinetic modelling of interleukin-1 receptor antagonist in plasma and cerebrospinal fluid of patients following subarachnoid haemorrhage. *Br. J. Clin. Pharmacol.* 65, 317–325. <https://doi.org/10.1111/j.1365-2125.2007.03026.x>.
Gutierrez, E.G., Banks, W.A., Kastin, A.J., 1994. Blood-borne interleukin-1 receptor antagonist crosses the blood–brain barrier. *J. Neuroimmunol.* 55, 153–160. [https://doi.org/10.1016/0165-5728\(94\)90005-1](https://doi.org/10.1016/0165-5728(94)90005-1).
Hannum, C.H., Wilcox, C.J., Arend, W.P., Joslin, F.G., Dripps, D.J., Heimdal, P.L., Armes, L.G., Sommer, A., Eisenberg, S.P., Thompson, R.C., 1990. Interleukin-1 receptor antagonist activity of a human interleukin-1 inhibitor. *Nature* 343, 336–340. <https://doi.org/10.1038/343336a0>.
Helms, H.C., Abbott, N.J., Burek, M., Cecchelli, R., Couraud, P.-O., Deli, M.A., Förster, C., Galla, H.J., Romero, I.A., Shusta, E.V., Stebbins, M.J., Vandenhaute, E., Weksler, B., Brodin, B., 2016. *In vitro* models of the blood–brain barrier: an overview of commonly used brain endothelial cell culture models and guidelines for their use.

- J. Cerebr. Blood Flow Metabol. 36, 862–890. <https://doi.org/10.1177/0271678x16630991>.
- Helmy, A., Guilfoyle, M.R., Carpenter, K.L., Pickard, J.D., Menon, D.K., Hutchinson, P.J., 2014. Recombinant human interleukin-1 receptor antagonist in severe traumatic brain injury: a phase II randomized control trial. *J. Cerebr. Blood Flow Metabol.* 34, 845–851. <https://doi.org/10.1038/jcbfm.2014.23>.
- Hladky, S.B., Barrand, M.A., 2014. Mechanisms of fluid movement into, through and out of the brain: evaluation of the evidence. *Fluids Barriers CNS* 11 (26). <https://doi.org/10.1186/2045-8118-11-26>.
- Hutchinson, P.J., O'Connell, M.T., Rothwell, N.J., Hopkins, S.J., Nørtje, J., Carpenter, K.L.H., Timofeev, I., Al-Rawi, P.G., Menon, D.K., Pickard, J.D., 2007. Inflammation in human brain injury intracerebral concentrations of IL-1, IL-1, and their endogenous inhibitor IL-1ra. *J. Neurotrauma* 24, 1545–1557. <https://doi.org/10.1089/neu.2007.0295>.
- Keizer, R.J., Huitema, A.D.R., Schellens, J.H.M., Beijnen, J.H., 2010. Clinical pharmacokinetics of therapeutic monoclonal antibodies. *Clin. Pharmacokinet.* 49, 493–507. <https://doi.org/10.2165/11531280-000000000-00000>.
- Kenney-Jung, D.L., Vezzani, A., Kahoud, R.J., LaFrance-Corey, R.G., Ho, M., Muskardian, T.W., Wirrell, E.C., Howe, C.L., Payne, E.T., 2016. Febrile infection-related epilepsy syndrome treated with anakinra. *Ann. Neurol.* 80, 939–945. <https://doi.org/10.1002/ana.24806>.
- Kineret Summary of Product Characteristics, 2020. Swedish orphan Biovitrum AB (publ). EMA. <https://www.ema.europa.eu/en/medicines/human/EPAR/kineret>.
- Koh, S., Wirrell, E., Vezzani, A., Nabbout, R., Muscal, E., Kaliaatsos, M., Wickström, R., Riviello, J.J., Brunklaus, A., Payne, E., Valentini, A., Wells, E., Carpenter, J.L., Lee, K., Lai, Y., Eschbach, K., Press, C.A., Gorman, M., Stredny, C.M., Roche, W., Mangum, T., 2021. Proposal to optimize evaluation and treatment of Febrile infection-related epilepsy syndrome (FIREs): a Report from FIREs workshop. *Epilepsia Open* 6, 62–72. <https://doi.org/10.1002/epi4.12447>.
- Konsman, J.P., Vigues, S., Mackerlova, L., Bristow, A., Blomqvist, A., 2004. Rat brain vascular distribution of interleukin-1 type-1 receptor immunoreactivity: relationship to patterns of inducible cyclooxygenase expression by peripheral inflammatory stimuli. *J. Comp. Neurol.* 472, 113–129. <https://doi.org/10.1002/cne.20052>.
- Kumar, R.G., Boles, J.A., Wagner, A.K., 2015. Chronic inflammation after severe traumatic brain injury. *J. Head Trauma Rehabil.* 30, 369–381. <https://doi.org/10.1097/htr.000000000000067>.
- Lazovic, J., Basu, A., Lin, H.-W., Rothstein, R.P., Krady, J.K., Smith, M.B., Levison, S.W., 2005. Neuroinflammation and both cytotoxic and vasogenic edema are reduced in interleukin-1 type 1 receptor-deficient mice conferring neuroprotection. *Stroke* 36, 2226–2231. <https://doi.org/10.1161/01.str.0000182255.08162.6a>.
- Liberale, L., Bonetti, N.R., Puspitasari, Y.M., Schwarz, L., Akhmedov, A., Montecucco, F., Ruschitzka, F., Beer, J.H., Lüscher, T.F., Simard, J., Libby, P., Camici, G.G., 2020. Postischemic administration of IL-1 α neutralizing antibody reduces brain damage and neurological deficit in experimental stroke. *Circulation* 142, 187–189. <https://doi.org/10.1161/circulationaha.120.046301>.
- Liebner, S., Dijkhuizen, R.M., Reiss, Y., Plate, K.H., Agalliu, D., Constantin, G., 2018. Functional morphology of the blood–brain barrier in health and disease. *Acta Neuropathol.* 135, 311–336. <https://doi.org/10.1007/s00401-018-1815-1>.
- Löscher, W., Friedman, A., 2020. Structural, molecular, and functional alterations of the blood-brain barrier during epileptogenesis and epilepsy: a cause, consequence, or both? *Int. J. Mol. Sci.* 21 (591). <https://doi.org/10.3390/ijms21020591>.
- Luheshi, N.M., Kovács, K.J., Lopez-Castejon, G., Brough, D., Denes, A., 2011. Interleukin-1 α expression precedes IL-1 β after ischemic brain injury and is localised to areas of focal neuronal loss and penumbral tissues. *J. Neuroinflammation* 8 (186). <https://doi.org/10.1186/1742-2094-8-186>.
- Maysami, S., Wong, R., Pradillo, J.M., Denes, A., Dhungana, H., Malm, T., Koistinaho, J., Orset, C., Rahman, M., Rubio, M., Schwanninger, M., Vivien, D., Bath, P.M., Rothwell, N.J., Allan, S.M., 2015. A cross-laboratory preclinical study on the effectiveness of interleukin-1 receptor antagonist in stroke. *J. Cerebr. Blood Flow Metabol.* 36, 596–605. <https://doi.org/10.1177/0271678x15606714>.
- McCann, S.K., Cramond, F., Macleod, M.R., Sena, E.S., 2016. Systematic review and meta-analysis of the efficacy of interleukin-1 receptor antagonist in animal models of stroke: an update. *Transl Stroke Res* 7, 395–406. <https://doi.org/10.1007/s12975-016-0489-z>.
- Murray, K.N., Parry-Jones, A.R., Allan, S.M., 2015. Interleukin-1 and acute brain injury. *Front. Cell. Neurosci.* 9 (18). <https://doi.org/10.3389/fncel.2015.00018>.
- Newell, E.A., Todd, B.P., Mahoney, J., Pieper, A.A., Ferguson, P.J., Bassuk, A.G., 2018. Combined blockade of interleukin-1 α and β signaling protects mice from cognitive dysfunction after traumatic brain injury. *Eneuro* 5, ENEURO 17–385. <https://doi.org/10.1523/eneuro.0385-17.2018>, 2018.
- Ozen, I., Ruscher, K., Nilsson, R., Flygt, J., Clausen, F., Marklund, N., 2020. Interleukin-1 beta neutralization attenuates traumatic brain injury-induced microglia activation and neuronal changes in the globus pallidus. *Int. J. Mol. Sci.* 21 (387). <https://doi.org/10.3390/ijms21020387>.
- Pardridge, W.M., 2012. Drug transport across the blood–brain barrier. *J. Cerebr. Blood Flow Metabol.* 32, 1959–1972. <https://doi.org/10.1038/jcbfm.2012.126>.
- Payne, E., Koh, S., Wirrell, E., 2020. Extinguishing febrile infection-related epilepsy syndrome: pipe dream or reality? *Semin. Neurol.* 40, 263–272. <https://doi.org/10.1055/s-0040-1708503>.
- Pedroso, D., Tellechea, A., Moura, L., Fidalgo-Carvalho, I., Duarte, J., Carvalho, E., Ferreira, L., 2011. Improved survival, vascular differentiation and wound healing potential of stem cells Co-cultured with endothelial cells. *PLoS One* 6, e16114. <https://doi.org/10.1371/journal.pone.0016114>.
- Pinteaux, E., Parker, L.C., Rothwell, N.J., Luheshi, G.N., 2002. Expression of interleukin-1 receptors and their role in interleukin-1 actions in murine microglial cells. *J. Neurochem.* 83, 754–763. <https://doi.org/10.1046/j.1471-4159.2002.01184.x>.
- Poduslo, J.F., Curran, G.L., Berg, C.T., 1994. Macromolecular permeability across the blood-nerve and blood-brain barriers. *Proc. Natl. Acad. Sci. Unit. States Am.* 91, 5705–5709. <https://doi.org/10.1073/pnas.91.12.5705>.
- Pradillo, J.M., Murray, K.N., Coutts, G.A., Moraga, A., Oroz-Gonjar, F., Boutin, H., Moro, M.A., Lizaola, I., Rothwell, N.J., Allan, S.M., 2017. Reporative effects of interleukin-1 receptor antagonist in young and aged/co-morbid rodents after cerebral ischemia. *Brain Behav. Immun.* 61, 117–126. <https://doi.org/10.1016/j.bbi.2016.11.013>.
- Relton, J.K., Martin, D., Thompson, R.C., Russell, D.A., 1996. Peripheral administration of interleukin-1 receptor antagonist inhibits brain damage after focal cerebral ischemia in the rat. *Exp. Neurol.* 138, 206–213. <https://doi.org/10.1006/exnr.1996.0059>.
- Sakuma, H., Tanuma, N., Kuki, I., Takahashi, Y., Shiomi, M., Hayashi, M., 2015. Intrathecal overproduction of proinflammatory cytokines and chemokines in febrile infection-related refractory status epilepticus. *J. Neurol. Neurosurg. Psychiatr.* 86 (820). <https://doi.org/10.1136/jnnp-2014-309388>.
- Shah, D.K., Betts, A.M., 2013. Antibody biodistribution coefficients. *Mabs* 5, 297–305. <https://doi.org/10.4161/mabs.23684>.
- Sibley, C.H., Chioato, A., Felix, S., Colin, L., Chakraborty, A., Plass, N., Rodriguez-Smith, J., Brewer, C., King, K., Zalewski, C., Kim, H.J., Bishop, R., Abrams, K., Stone, D., Chapelle, D., Kost, B., Snyder, C., Butman, J.A., Wesley, R., Goldbach-Mansky, R., 2015. A 24-month open-label study of canakinumab in neonatal-onset multisystem inflammatory disease. *Ann. Rheum. Dis.* 74 (1714). <https://doi.org/10.1136/annrheumdis-2013-204877>.
- Sibley, C.H., Plass, N., Snow, J., Wiggs, E.A., Brewer, C.C., King, K.A., Zalewski, C., Kim, H.J., Bishop, R., Hill, S., Paul, S.M., Kicker, P., Phillips, Z., Dolan, J.G., Widemann, B., Jayaprakash, N., Cucino, F., Stone, D.L., Chapelle, D., Snyder, C., Butman, J.A., Wesley, R., Goldbach-Mansky, R., 2012. Sustained response and prevention of damage progression in patients with neonatal-onset multisystem inflammatory disease treated with anakinra: a cohort study to determine three- and five-year outcomes. *Arthritis Rheum.* 64, 2375–2386. <https://doi.org/10.1002/art.34409>.
- Skinner, R., Gibson, R., Rothwell, N., Pinteaux, E., Penny, J., 2009. Transport of interleukin-1 across cerebrovascular endothelial cells. *Br. J. Pharmacol.* 156, 1115–1123. <https://doi.org/10.1111/j.1476-5381.2008.00129.x>.
- Vandenhoute, E., Drolez, A., Sevin, E., Gosselet, F., Mysiorek, C., Dehouck, M.-P., 2016. Adapting coculture in vitro models of the blood–brain barrier for use in cancer research: maintaining an appropriate endothelial monolayer for the assessment of transendothelial migration. *Lab. Invest.* 96, 588–598. <https://doi.org/10.1038/labinvest.2016.35>.
- Vezzani, A., French, J., Bartfai, T., Baram, T.Z., 2011. The role of inflammation in epilepsy. *Nat. Rev. Neurol.* 7, 31–40. <https://doi.org/10.1038/nrneuro.2010.178>.
- Webster, K.M., Sun, M., Crack, P., O'Brien, T.J., Shultz, S.R., Semple, B.D., 2017. Inflammation in epileptogenesis after traumatic brain injury. *J. Neuroinflammation* 14 (10). <https://doi.org/10.1186/s12974-016-0786-1>.
- Westbrook, C., Subramaniam, T., Seagren, R.M., Tarula, E., Co, D., Furstenberg-Knauff, M., Wallace, A., Hsu, D., Payne, E., 2019. Febrile infection-related epilepsy syndrome treated successfully with anakinra in a 21-year-old woman. *Wmj Official Publ State Medical Soc Wis* 118, 135–139.
- Whiteley, W., Jackson, C., Lewis, S., Lowe, G., Rumley, A., Sandercock, P., Wardlaw, J., Dennis, M., Sudlow, C., 2009. Inflammatory markers and poor outcome after stroke: a prospective cohort study and systematic review of interleukin-6. *PLoS Med.* 6, e1000145. <https://doi.org/10.1371/journal.pmed.1000145>.
- Yamasaki, Y., Matsuura, N., Shozuhara, H., Onodera, H., Itoyama, Y., Kogure, K., 1995. Interleukin-1 as a pathogenetic mediator of ischemic brain damage in rats. *Stroke* 26, 676–681. <https://doi.org/10.1161/01.str.26.4.676>.